International Conference on Nuclear Data for Science and Technology 2007
DOI: 10.1051/ndata:07571

Evaluation of iridium (n,xn) reactions

S. Cowell[a], P. Talou[b], T. Kawano, and M.B. Chadwick

Nuclear Physics Group, Los Alamos National Laboratory, Los Alamos, NM 87545, USA

Abstract. Recent experimental data, including detailed studies of the ^{191}Ir and ^{193}Ir metastable states have significantly improved our understanding of the nuclear structure for many iridium isotopes. Combining experimental γ production cross sections with the results of the reaction theory code GNASH, improved evaluations of neutron induced cross sections on several iridium isotopes have been completed. With a focus on improved descriptions of nuclear structure and pre-equilibrium modeling, ^{191}Ir(n, xn) cross sections are presented.

1 Introduction

Iridium (Ir) isotopes are used in a variety of medical and industrial applications, ranging from cancer treatment to activation detectors used to probe the energy spectrum of a neutron fluence. Their efficacy often depends on a complete understanding of (n, xn) cross sections. The nuclear structure of Ir includes several isomeric states whose production cross sections are difficult to probe experimentally and evaluated cross section are required. GNASH calculations, based on the compound nucleus theory of Hauser-Feshbach, can be used to predict the relevant cross sections. However, GNASH relies heavily on the low-energy nuclear structure as input. Until recently, this structure was not well known for several Ir isotopes. Recent experimental data, including detailed studies of the ^{191}Ir and ^{193}Ir metastable states obtained using the GEANIE (GErmanium Array for Neutron Induced Excitations) detector at the Los Alamos Neutron Science Center (LANSCE) [1,2], significantly improved our understanding of the nuclear structure using the (n, n$'\gamma$) reaction in ^{191}Ir and ^{193}Ir. In addition, several theoretical improvements to GNASH have been incorporated in recent years [3], most significant of which is the pre-equilibrium Feshbach-Kerman-Koonin (FKK) single-step reaction model [4] used to obtain the spin distribution of the residual nucleus. Utilizing γ production cross sections obtained by GEANIE, improved GNASH evaluations of neutron cross sections on Ir isotopes have been performed. Section 2 briefly describes the models employed in the GNASH evaluations. Section 3 presents results for the isomer production cross section, ^{191}Ir(n, 2n)^{190}Ir and ^{191}Ir(n, xn) reactions.

2 GNASH Evaluation

GNASH calculations [5], based on the compound nucleus theory of Hauser-Feshbach (HF), were performed to obtain γ-ray production cross sections. In HF, a compound nucleus (CN) is produced by a projectile incident on a target. Provided that the CN is long enough lived to have reached equilibrium, the properties and decay of the compound system (with the exception of conserved quantities such as energy, spin, parity and particle number) do not depend on the entrance channel that produced it. The formation and decay of the CN are independent of each other. Accordingly, the partial compound reaction cross section is factorized into the formation cross section from the entrance channel, and the probability for the decays of the CN to the final channel.

From equilibrium, the CN decays via a series of γ and particle emissions. Through each step of the decay, level populations for all nuclear states present in the decay chain are calculated by GNASH. Once the CN is fully de-excited, these populations determine the γ-ray and particle emission cross sections.

Though HF has proved to be a suitable model when the CN is in equilibrium, particle emission prior to the composite system coming to equilibrium must be incorporated. Several corrections to HF have been incorporated into GNASH including direct reactions as well as pre-equilibrium emissions occurring at high energies. The later effects are often accounted for using either a semi-classical exciton model or, more recently, the quantum mechanical theory of Feshbach-Kerman-Koonin (FKK) [4]. The original FKK theory is a multi-step model. At this time, GNASH employs only the dominant single-step direct component. Direct reactions are calculated using coupled-channels theory.

The present GNASH calculation of ^{191}Ir cross sections utilizes transmission coefficients for the HF calculations obtained using a coupled channels optical potential. The γ-ray strength functions (or transmission coefficients) were approximated using the Kopecky and Uhl model [6] which utilizes a generalized Lorentzian form for the $E1$ strength function. Giant dipole resonance methods are employed for $E2$ and $M1$ strength functions. Continuum level densities are approximated using Ignatyuk et al. [7]. We compare exciton and one-step FKK (FKK-GNASH) pre-equilibrium model evaluations.

GNASH results are sensitive to the nuclear structure input for reaction chain nuclei. Presently available data were augmented/modified using absolute partial γ-ray cross sections provided by GEANIE. When possible, branching ratios, and

[a] Presenting author, e-mail: scowell@lanl.gov
[b] Present address: DEN/DER/SPRC/LEPh, CEA Cadarache, France

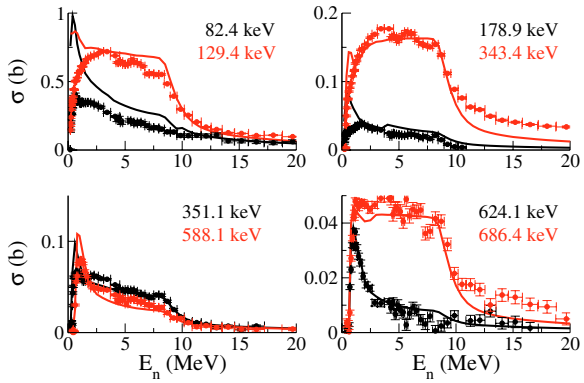

Fig. 1. γ production cross sections obtained by GEANIE are compared with FKK-GNASH calculations for several γ transitions to the ground state of ^{191}Ir. In general, the data are well reproduced.

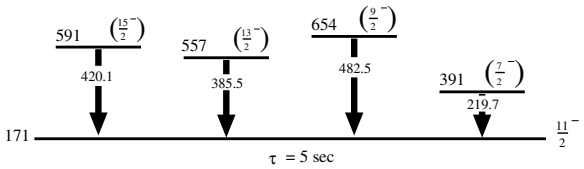

Fig. 2. Dominant γ-ray transitions feeding the 11/2− isomer state of ^{191}Ir.

J^{π} values were chosen to best reproduce experimental data. In general, available data are well reproduced. Figure 1 compares several FKK-GNASH and GEANIE data for the strongest direct transitions to the ground state of ^{191}Ir after neutron inelastic scattering.

3 Results

3.1 ^{191}Ir(n,n′)^{191m}Ir

^{191}Ir has a high-spin isomer state at 171 keV. GEANIE observed four γ transitions feeding directly this metastable state (see fig. 2). The branching ratios used as input to GNASH were adjusted to provide the best fit to data for these four transitions. Figure 3 compares the FKK-GNASH (solid) and exciton (dash) cross section evaluations to GEANIE data. Production cross sections are sensitive to the spin distribution of the residual nucleus as determined by the pre-equilibrium reactions. Both models give similar results for the transitions from low-spin states (482.5 and 219.7 keV). However, the semi-classical exciton model, which does not calculate spin transfer, overestimates the population of high-spin states and therefore yields significantly larger high-energy cross sections for the 385.5 and 420.1 keV transitions. Both models under predict the 482.5 keV transition from the $\left(\frac{9}{2}^{-}\right)$ 654 keV state; indicating inaccuracies in the nuclear structure input.

The sum of the γ-ray production cross sections for these four transitions accounts for most of the ^{191}Ir(n, n′)^{191m}Ir production cross section as can be seen in figure 4. Despite some inaccuracies in the individual cross sections shown in figure 3, the sum of these transitions is well reproduced by

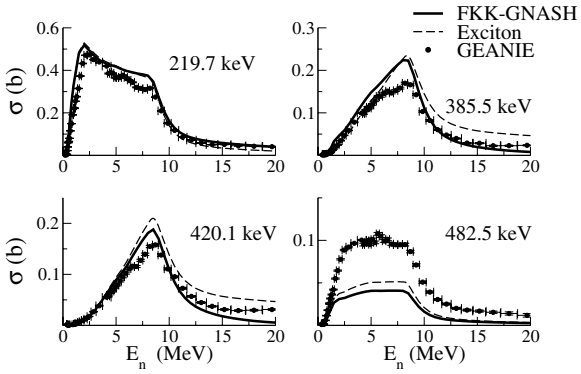

Fig. 3. γ production cross sections for the four dominant γ-ray transitions to the $\frac{11}{2}^{-}$ 171 keV isomer of ^{191}Ir. Evaluations obtained using the FKK-GNASH (solid) and exciton (dash) models are compared with GEANIE data.

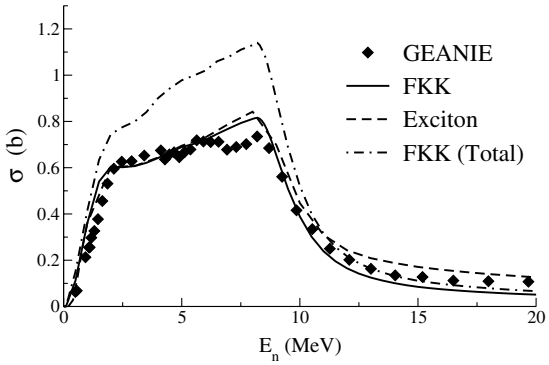

Fig. 4. Isomer production cross section of ^{191}Ir. Partial isomer production data (diamonds) is well reproduced by FKK-GNASH (dash) and exciton (solid) evaluations. The dash-dot line indicates the total ^{191}Ir(n, n′)^{191m}Ir cross section predicted by FKK-GNASH.

both the exciton (dash) and FKK-GNASH (solid) evaluations. However, the exciton evaluation overestimates, where the FKK-GNASH slightly under predicts the data at higher energies. There may be multiple-scattering events that have not been included in the analysis of the GEANIE data. If this experimental effect is large, this is expected to decrease the high-energy tail bringing FKK-GNASH and GEANIE into better agreement. We limit further discussions of (n, xn) cross sections to those obtained using FKK-GNASH.

3.2 Partial ^{191}Ir(n,2n)^{190}Ir

^{190}Ir has multiple isomer states (see fig. 5). Previous ENDF evaluations [8] of ^{191}Ir(n,2n)^{190}Ir did not incorporate the short-lived 36.2 keV isomer. Combining experimental data of Garrett [2] and GEANIE, we were able to compute the production cross section for this isomer state. Figure 6 shows two of the strongest transitions to the "m2" state; FKK-GNASH well reproduces the GEANIE data.

Note that the 376 keV "m3" isomer decays 91.4% of the time via electron capture and 8.6% via internal conversion. Activation experiments are sensitive to the m3 decay structure

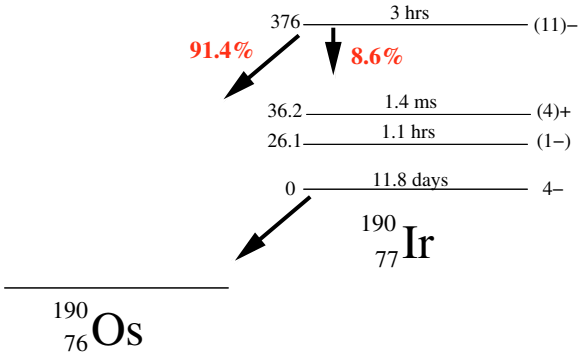

Fig. 5. Isomer states of ^{190}Ir.

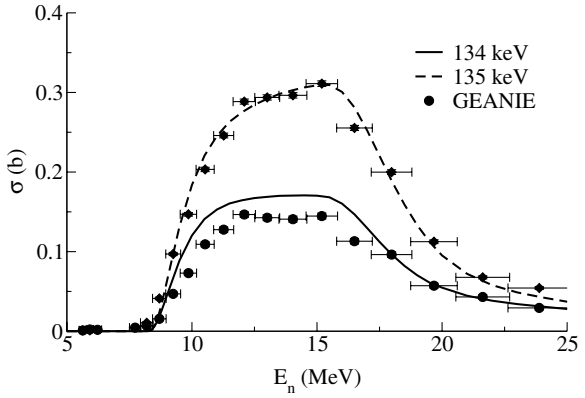

Fig. 6. FKK-GNASH (solid) and GEANIE production cross sections for the 134 and 135 keV transitions to the 36.1 keV isomer states of ^{190}Ir.

and it is inappropriate to compare these experimental results with total (n, 2n) evaluated cross sections. A modified sum of the individual excitation functions:

$$^{191}\mathrm{Ir(n,2n)}\left[^{190g}\mathrm{Ir} + {}^{190m1}\mathrm{Ir} + {}^{190m2}\mathrm{Ir} + 0.086\,{}^{190m3}\mathrm{Ir}\right],$$

which accounts for the depletion of the m3 isomer, best mimics the experimental scenario. Figure 7 shows the individual excitation functions for ^{190g}Ir (dash) and ^{190m1,m2,m3}Ir (dot, dot-dash and double dot-dash respectively). Experimental data are available only for ^{191}Ir(n, 2n)^{190m3}Ir (diamonds) [9–14]. The FKK-GNASH m3 production cross section agrees within ∼15%. The FKK-GNASH sum (solid) compares well with experiment [11, 15–17].

3.3 Total ^{191}Ir(n,xn)

Total (n, xn) cross section as determined by FKK-GNASH are shown in figure 8. For comparison, we provide experimental data from Bayhurst et al. [15].

3.4 ENDF

We have produced a new ENDF file associated with the presented evaluation including uncertainty quantification not

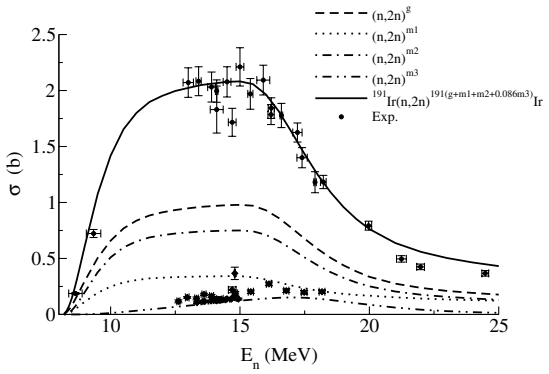

Fig. 7. Evaluated ground state (dashed) and isomer (m1-dot; m2-dot-dash; m3-double dot-dash) production cross sections. ^{191}Ir(n, 2n)$^{191(g+m1+m2+0.086m3)}$Ir (solid) agrees well with experimental (n, 2n) data. See text for further explanation.

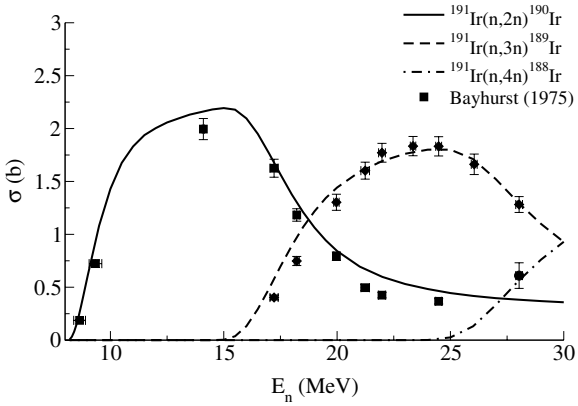

Fig. 8. FKK-GNASH and experimental [15] ^{191}Ir(n, xn) cross sections.

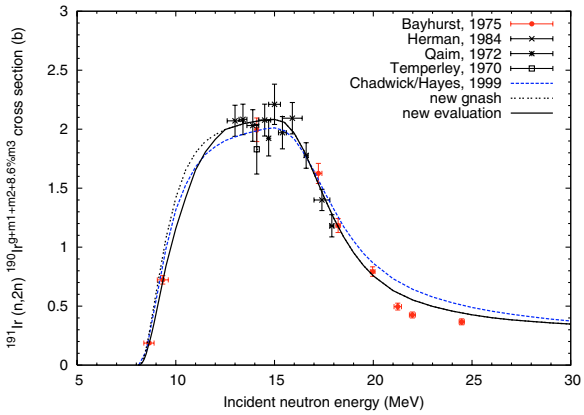

Fig. 9. Evaluated ^{191}Ir(n, 2n)$^{191(g+m1+m2+0.086m3)}$Ir (dotted) and evaluation (with modifications) (solid) are compared with experiment and previous calculations (dash).

discussed here [19]. Though the ^{191}Ir(n,2n)^{190}Ir evaluation described above agrees reasonably well with experiment, some modifications were made to the FKK-GNASH evaluation to better represent the threshold data. A slight adjustment below 10 MeV was made to better agree with the 9.34 MeV Bayhurst data point. In addition, the m3 isomer population cross section

was increased by a normalization factor of 1.205 to better predict available data (see fig. 7). This modified FKK-GNASH evaluation is shown in figure 9 and compared with previous evaluations [18] and experiment.

We would like to thank N Fotiades, R.O. Nelson, M. Devlin, J.A. Becker, and L.A Bernstein for the GEANIE experimental data.

References

1. N. Fotiades et al., *Proceedings of the International Conference on Nuclear Data for Science and Technology, Santa Fe, 2004*, edited by R.C. Haight, M.B. Chadwich, T. Kawano, P. Talou (AIP Conference Proceedings CP769, 2005) 898.
2. P.E. Garrett et al., Nucl. Phys. A **611**, 68 (1996).
3. D. Dashdorj et al., Phys. Rev. C (to be published).
4. H. Feshbach, A. Kerman, S. Koonin, Ann. Phys. (NY) **125**, 429 (1980).
5. P.G. Young, E.D. Arthur, M.B. Chadwick, Los Alamos National Laboratory report No. LA-UR-96-3739.
6. J. Kopecky, M. Uhl, Phys. Rev. C **42**, 1941 (1990).
7. A.V. Ignatyuk, G.N. Smirenkin, A.S. Tishin, Sov. J. Nucl. Phys. **21**, 255 (1975).
8. P. Talou (private communication).
9. A.A. Filatenkov, S.V. Chuvaev, Khlopin Radiev. Inst., Leningrad Reports No. 259 (2003).
10. C. Konno, Y. Ikeda, K. Oishi, K. Kawade, H. Yamamoto, H. Maekawa, JAERI Reports No. 1329 (1993).
11. M. Herman, A. Marcinkowski, K. Stankiewicz, Nucl. Phys. A **430**, 69 (1984).
12. M. Herman, A. Marcinkowski, IAEA Nucl. Data Section Report to the I.N.D.C. No. 103, 40 (1979).
13. M. Bormann, H.H. Bissem, E. Magiera, R. Warnemunde, Nucl. Phys. A **157**, 481 (1970).
14. C.S. Khurana, H.S. Hans, Nucl. Phys. **28**, 560 (1961).
15. B.P. Bayhurst, J.S. Gilmore, R.J. Prestwood, J.B. Wilhelmy, N. Jarmie, B.H. Erkkila, R.A. Hardekopf, Phys. Rev. C **12**, 451 (1973).
16. S.M. Qaim, Nucl. Phys. A **185**, 614 (1972).
17. J.K. Temperley, D.E. Barnes, Ballistic Research Labs Reports, No. 1491, (1970).
18. M.B. Chadwick, A.C. Hayes, LA-CP-99-226 (1999).
19. P. Talou et al., LA-UR-06-4956 (2006).